Available online at www.sciencedirect.com
ScienceDirect
Journal of Solid State Chemistry 180 (2007) 3001–3007
JOURNAL OF SOLID STATE CHEMISTRY
www.elsevier.com/locate/jssc

# Structures and crystal chemistry of the double perovskites $Ba_2LnB'O_6$ ($Ln$ = lanthanide and $B'$ = Nb, Ta): Part II—Temperature dependence of the structures of $Ba_2LnB'O_6$

Paul J. Saines[a], Jarrah R. Spencer[a], Brendan J. Kennedy[a,*], Yoshiki Kubota[b], Chiharu Minakata[b], Hiroko Hano[b], Kenichi Kato[c], Masaki Takata[c]

[a]*School of Chemistry, The University of Sydney, Sydney, NSW 2006, Australia*
[b]*Department of Physical Science, Graduate School of Science, Osaka Prefecture University, Sakai, Osaka 599-8531, Japan*
[c]*RIKEN SPring-8 Center, 1-1-1 Kouto, Sayo-cho, Sayo-gun, Hyogo 679-5148, Japan*

Received 25 May 2007; received in revised form 5 August 2007; accepted 10 August 2007
Available online 28 August 2007

**Abstract**

The structures of eight members of the series of double perovskites of the type $Ba_2LnB'O_6$ ($Ln = La^{3+}$–$Sm^{3+}$ and $Y^{3+}$ and $B' = Nb^{5+}$ and $Ta^{5+}$) were examined both above and below room temperature using synchrotron X-ray powder diffraction. The $La^{3+}$ and $Pr^{3+}$ containing compounds had an intermediate rhombohedral phase whereas the other tantalates and niobates studied have a tetragonal intermediate. This difference in symmetry appears to be a consequence of the larger size of the $La^{3+}$ and $Pr^{3+}$ cations compared to the other lanthanides. The temperature range over which the intermediate symmetry is stable is reduced in those compounds near the point where the preferred intermediate symmetry changes from tetragonal to rhombohedral. In such compounds the transition to the cubic phase involves higher order terms in the Landau expression. This suggests that in this region the stability of the two intermediate phases is similar.


*Keywords:* Perovskite; Phase transition; Neutron powder diffraction; Synchrotron X-ray powder diffraction

## 1. Introduction

The precise structures adopted by various members of the family of double perovskite-type oxides $Ba_2LnB'O_6$ ($Ln$ = lanthanides and $Y^{3+}$ and $B' = Nb^{5+}$, $Ta^{5+}$, $Mo^{5+}$, $Ru^{5+}$, $Ir^{5+}$, $Sb^{5+}$ and $Bi^{5+}$) have been the focus of considerable recent attention [1–8]. These oxides exhibit a series of phase transitions dependent upon the size of the lanthanide ion. As the lanthanide ion gets smaller, the volume of the $AO_{12}$ polyhedron becomes better matched to the volume of the average $BO_6$ octahedron reducing the need for the octahedral tilting. Octahedral tilting can also be reduced by heating the sample.

The majority of the $Ba_2LnB'O_6$ double perovskites have either a monoclinic $I2/m$ (Glazer [9,10] tilt system $a^-a^-c^0$) or cubic $Fm\bar{3}m$ ($a^0a^0a^0$) structure. A smaller number exhibits either a rhombohedral $R\bar{3}$ ($a^-a^-a^-$) or $I4/m$ tetragonal ($a^0a^0c^-$) structure which can be viewed as an intermediate phase between the $I2/m$ and $Fm\bar{3}m$ end members. The $d$-electron configuration of the $B'$-site cation appears to have a significant influence of which of these two intermediate phases is formed [1]. When only a small number of $d$-electrons are present tetragonal symmetry is favored. Consistent with this in, Part I of this work, it was shown that at room temperature the tantalate oxides $Ba_2LnTaO_6$ have the tetragonal structure for the intermediate sized lanthanides $Sm^{3+}$–$Dy^{3+}$.

In the same paper, variable temperature neutron diffraction data showed that $Ba_2LaTaO_6$ undergoes a series of phase transitions with increasing temperature involving the rhombohedral, rather than tetragonal intermediate phase [11]. The reason for this was unclear, and it was suggested that this could possibly be caused by either

*Corresponding author. Fax: +61 2 9351 3329.
*E-mail address:* kennedyb@chem.usyd.edu.au (B.J. Kennedy).

0022-4596/$ - see front matter © 2007 Elsevier Inc. All rights reserved.
doi:10.1016/j.jssc.2007.08.010

the larger size of $La^{3+}$ cation compared to the other trivalent lanthanides or as a result of $La^{3+}$ not having any *f*-electrons. Since the niobates are expected to exhibit similar structures to the tantalates it is worth establishing if the rhombohedral phase also exists in $Ba_2LaNbO_6$ or in any of the other tantalates and niobates for which the intermediate structure is yet to be established.

To fully elucidate the sequence of structures adopted by various members of the $Ba_2LnNbO_6$ and $Ba_2LnTaO_6$ series, and determine which of the two possible intermediates they adopt, we have examined these structures both above and below room temperature using synchrotron X-ray diffraction. Synchrotron X-ray diffraction has been chosen due to its high resolution, which allows splitting of the diagnostic peaks to be identified, and also due to its higher intensity, which allows better examination of weak reflections. Both of these factors allow more precise determination of the symmetry of the perovskites studied in this work and in particular which of the two intermediate symmetries is adopted.

## 2. Experimental

The method for preparing these compounds is as described in either the work of Saines et al. [1] in the case of the niobium compounds or in Part I of this work [11] in the case of the tantalates.

Synchrotron X-ray powder diffraction data for $Ba_2LnB'O_6$ ($Ln = La^{3+}$, $Pr^{3+}$, $Nd^{3+}$ and $Sm^{3+}$ and $B' = Nb^{5+}$ and $Ta^{5+}$) both at and above room temperature were recorded on the Debye–Scherrer diffractometer at the Australian National Beamline Facility, Beamline 20B at the Photon Factory, Tsukuba, Japan [12]. The samples were heated up to a maximum of 1073 K using a custom built furnace and were housed in 0.3 mm quartz capillaries that were continuously rotated during measurement to improve particle averaging and to reduce the effects of preferred orientation. It took approximately 10 min to reach thermal equilibrium at each temperature. Data were collected using two image plates as detectors covering the range of approximately $5 < 2\theta < 85^\circ$ with a step size of $0.01^\circ$ and a wavelength of 0.80088(1) Å, 0.80123(1) Å or 0.80286(1) Å.

High-resolution synchrotron X-ray diffraction patterns were recorded of $Ba_2LnTaO_6$ ($Ln = La^{3+}$ and $Y^{3+}$) at temperatures between 90 and 300 K on the Debye–Scherrer diffractometer on BL-02B2 at SPring-8 [13]. Data were collected using 0.6000(1) Å X-rays. The samples were sealed in 0.2 mm diameter glass capillaries and were rotated during the measurements. Data were collected at angles of up to $85^\circ$ using a single Fuji image plate as the detector. The samples were cooled using a liquid nitrogen cryostream with the temperature held to within $\pm 1^\circ$ of the set point during the measurements. Samples were allowed 5 min to reach thermal equilibrium between measurements.

Refinements of the crystal structures were performed using the program RIETICA [14]. The diffraction peaks were described by a pseudo-Voight function using a Howard asymmetry correction where necessary [14]. The background was estimated from interpolation between up to 40 selected points.

## 3. Results and discussion

### 3.1. Variable temperature structures of $Ba_2LnB'O_6$

The crystal structure of $Ba_2LaTaO_6$ was examined over the temperature range 90–898 K using synchrotron X-ray diffraction. As found in Part I of this work [11], the X-ray diffraction patterns revealed a phase transition from $I2/m$ monoclinic (tilt system $a^-a^-c^0$) to $R\bar{3}$ rhombohedral ($a^-a^-a^-$) near room temperature. Further heating of the sample revealed another transition to $Fm\bar{3}m$ cubic symmetry ($a^0a^0a^0$) (see Fig. 1).

The phase transition between the monoclinic and rhombohedral phases is discontinuous as indicated by the large two-phase region which starts at 140 K and ends in the range 300–398 K (see Fig. 2). The precise upper temperature limit of this two-phase region could not be established due to the need to change set-ups between the high- and low-temperature data collection. It should also be noted that there was a significant increase between the lattice parameter, *a*, measured at 300 and 400 K. This is presumably an artifact of using two different instruments to collect the below and above ambient temperature data. This necessitates the wavelength of each to be calibrated independently which can result in a slight discrepancy in the lattice parameter between the two measurements. The transition between the rhombohedral and cubic phases was continuous and, from the loss of resolved splitting in the diffraction patterns, was estimated to occur between 798 and 823 K. The spontaneous rhombohedral strain is proportional to both the rhombohedral distortion (α-60)

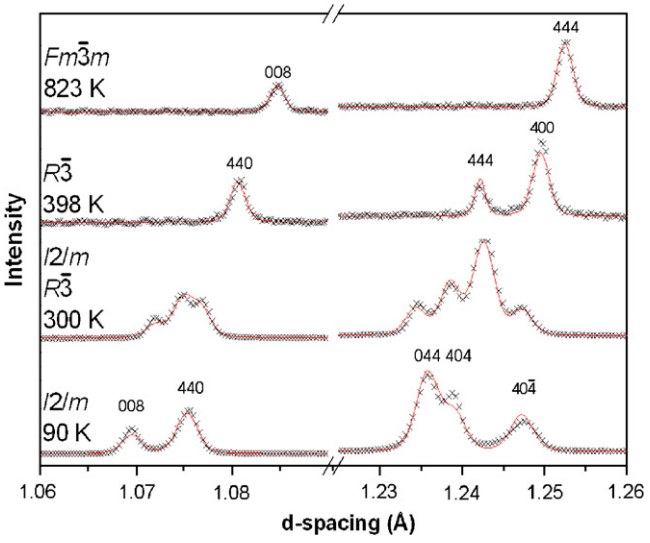


Fig. 1. Selected sections of diffraction patterns of $Ba_2LaTaO_6$ with changing temperature indicating the symmetry of the various structures found to be adopted.

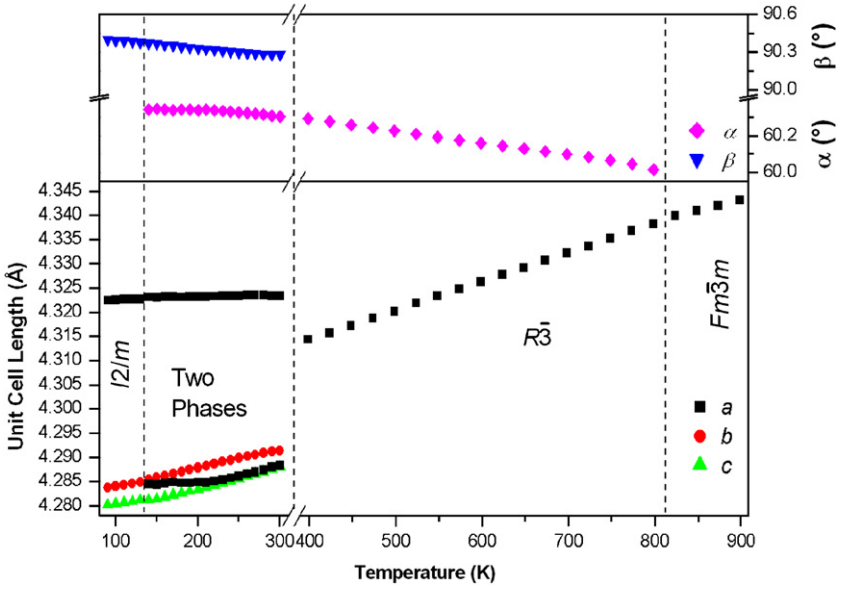


Fig. 2. Lattice parameters versus temperature for $Ba_2LaTaO_6$ indicating the sequence of phase transitions adopted with increasing temperature. The break in the data is caused by using two different diffractometers for collection of the diffraction patterns. The unit cell lengths have been reduced to the same size as a primitive cubic perovskite unit cell.

and also to the square of the order parameter ($Q^2$) [15]. A plot of the rhombohedral distortion versus temperature is observed to be linear indicating that the phase transition is second order (Fig. 3). Extrapolation of the plot to zero strain indicates that the phase transition should occur at 838(4) K. This value is significantly higher than the temperature estimated from the peak splitting and demonstrates the limitation of estimating phase transition temperatures using peak splitting where the instrument resolution may be insufficient to separate small splitting of peaks.

There is a small discrepancy between the results described here using synchrotron X-ray diffraction and our previous neutron diffraction study. The neutron diffraction study demonstrated that at 100 K the monoclinic phase is in $P2_1/n$ whereas the synchrotron X-ray diffraction pattern indicates $I2/m$ symmetry is appropriate. Despite the low background there was no evidence in the synchrotron X-ray diffraction pattern at 90 K for either *M*- or *X*-point reflections. Attempts to model this 90 K pattern using a structure in $P2_1/n$ resulted in a fit that was not significantly better than that obtained using $I2/m$ despite the six extra parameters allowed in the $P2_1/n$ model ($R_p$ and $R_{wp}$ of 4.2% and 5.7% for $I2/m$ respectively compared to 4.0% and 5.5% for $P2_1/n$). More critically the fit in $P2_1/n$ calculated intensities for some of the low angle *M*- and *X*-superlattice reflections that were not experimentally observed. Two possible reasons for this discrepancy are either, a small error in the temperature between the two measurements, or more likely, that the magnitude of the in-phase tilts that give rise to *M*- and *X*-point reflections is sufficiently small as to be undetected in the synchrotron measurement, and the Rietveld fit is overestimating this. A comparison of the diffraction pattern with a model with $P2_1/n$ symmetry generated using oxygen atomic positions determined from the neutron diffraction indicated that the *M*- and *X*-point superlattice reflections would be too weak to be seen above the background of the pattern. This is consistent with the structure of $Ba_2LaTaO_6$ being $P2_1/n$ under 100 K but the synchrotron data being insufficiently sensitive to the oxygen positions to be able to correctly refine this structure.

Having established the full sequence of phase transitions for $Ba_2LaTaO_6$, we studied the high-temperature transitions in some related $Ba_2LnB'O_6$ compounds. As observed for $Ba_2LaTaO_6$, $Ba_2LaNbO_6$ showed the sequence of phases $I2/m$ to $R\bar{3}$ and ultimately to $Fm\bar{3}m$ upon heating. The monoclinic and rhombohedral phases co-existed between 398 and 523 K indicating that transition between these was discontinuous. The phase transition from rhombohedral to cubic was continuous and occurs near 848 K based on the loss of peak splitting. This temperature is similar to the transition temperature found for $Ba_2LaTaO_6$. A plot of the rhombohedral distortion versus temperature was linear indicating that the rhombohedral to cubic phase transition in $Ba_2LaNbO_6$ is also second order with a transition temperature of 862(6) K.

Both $Ba_2PrNbO_6$ and $Ba_2PrTaO_6$ exhibit the same sequence of phase transitions seen for $Ba_2LaNbO_6$ and $Ba_2LaTaO_6$, however the rhombohedral phase persists over a smaller temperature range in the $Pr^{3+}$ oxides (Table 1). In the $La^{3+}$ compounds the rhombohedral phase is stable for between 300° and 500° while in the $Pr^{3+}$ compounds it is only seen for a little over 100°. Further the magnitude of the rhombohedral splitting is smaller in the $Pr^{3+}$ compounds than in the $La^{3+}$ compounds (Figs. 2 and 4). Again we find that, as expected, the monoclinic to rhombohedral

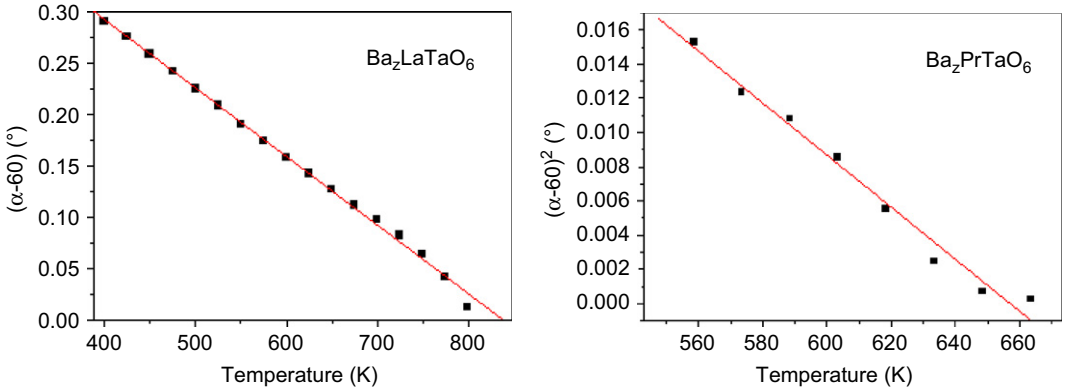


Fig. 3. Plot of rhombohedral distortion (as represented by (α-60) and rhombohedral distortion squared versus temperature plot for $Ba_2LaTaO_6$ and $Ba_2PrTaO_6$, respectively. The linear nature of these plots indicates that the rhombohedral to cubic phase transition is second order for $Ba_2LaTaO_6$ and tricritical for $Ba_2PrTaO_6$.

Table 1
Transition temperatures for the niobate and tantalate double perovskites, where a two-phase region of co-existence is noted by ~ and the data collected do not fully cover the range of phase co-existence

| Compound | Temperature range of two-phase co-existance of monoclinic and intermediate phases (K) | Transition temperature to cubic | |
|---|---|---|---|
| | | From splitting (K) | From strain (K) |
| $Ba_2LaNbO_6$ | ~398–523 | 823–848 | 862(6) |
| $Ba_2LaTaO_6$ | ~140–298 | 798–823 | 838(4) |
| $Ba_2PrNbO_6$ | 503–623 | 713–728 | –[a] |
| $Ba_2PrTaO_6$ | 453–528 | 663–678 | 656(3) |
| $Ba_2NdNbO_6$ | 508–628 | 688–698 | 695(2) |
| $Ba_2NdTaO_6$ | 523–598 | 698–723 | –[a] |
| $Ba_2SmNbO_6$ | ~298 | 573–598 | 582(1) |

[a]Insufficient temperatures were studied to complete a spontaneous Strain analysis.

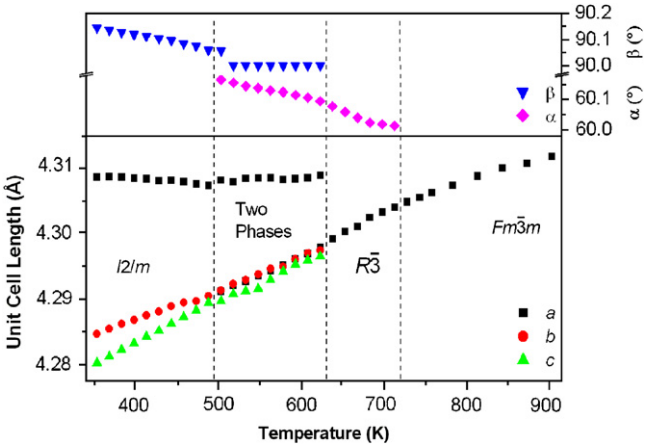


Fig. 4. Unit cell parameters versus temperature plot for $Ba_2PrNbO_6$ indicating the series of phase transitions adopted with increasing temperature.

and rhombohedral to cubic phase transitions in the $Pr^{3+}$ compounds are discontinuous and continuous, respectively (Fig. 4). A plot of the square of the spontaneous strain in $Ba_2PrTaO_6$ versus temperature is linear (Fig. 3) suggesting that this phase transition is tricritical with $T_c = 656(3)$ K. The limited temperature range over which the rhombohedral phase exists as a single phase limits the accuracy of this strain analysis somewhat. For a similar reason, we could not estimate the nature of the transition in $Ba_2PrNbO_6$ from the spontaneous strain.

As shown previously [1] $Ba_2NdNbO_6$ adopts a tetragonal, as opposed to rhombohedral, intermediate. $Ba_2NdTaO_6$ also adopts the tetragonal intermediate (see Fig. 5). For both oxides the monoclinic to tetragonal transition is discontinuous (as indicated by the presence of the two-phase region) and the tetragonal to cubic phase transition is continuous. The limited thermal stability of the tetragonal phase in $Ba_2NdTaO_6$ coupled with the relatively coarse intervals employed precludes analysis of the spontaneous strains. Since the tetragonal to cubic phase transition in $Ba_2NdNbO_6$ was found to be tricritical it is likely that this phase transition in $Ba_2NdTaO_6$ may also be tricritical. The temperature range over which the single-phase tetragonal structure exists in $Ba_2NdNbO_6$ and $Ba_2NdTaO_6$ is 75–100° (Table 1); which is significantly less than the range over which this phase exists in $Ba_2SmNbO_6$ ca. 200°. The tetragonal splitting is also larger in the $Sm^{3+}$ compound than in $Ba_2NdNbO_6$ or $Ba_2NdTaO_6$ ($a\sqrt{2}/c = 0.99597$ for $Ba_2SmNbO_6$ cf. 0.99824

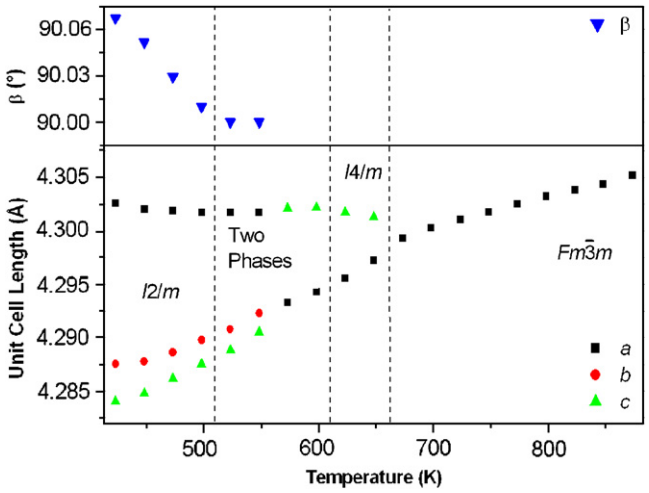


Fig. 5. Unit cell parameters versus temperature for $Ba_2NdTaO_6$ indicating the series of phase transitions adopted with increasing temperature. Only the lattice parameters of the major phase present in the two-phase region is illustrated.

and 0.99906 for $Ba_2NdNbO_6$ and $Ba_2NdTaO_6$ for the most distorted structure in a single-phase region).

The increased splitting and temperature range stability of the tetragonal phase in $Ba_2SmNbO_6$ compared to $Ba_2NdNbO_6$ and $Ba_2NdTaO_6$ is similar to the behavior of the rhombohedral structure in the $La^{3+}$ and $Pr^{3+}$ oxides; that is in the compounds closest to the point where the changeover between the intermediate symmetries occurs, the intermediate structure is less distorted and is seen over a limited temperature range. This suggests that near the changeover point the stability of the intermediate structure decreases. The contributions of the higher order terms of the Landau free energy expansion to the phase transition between the intermediate and cubic phases also increase as this change over point approaches. This work, and previous work by our group [1] indicates that the $La^{3+}$ compounds have a second-order phase transition varying as $Q^2$, the $Pr^{3+}$ and $Nd^{3+}$ compounds, for which it is possible to do a spontaneous strain analysis, appear to have a tricritical phase transition varying as $Q^4$ and $Ba_2SmNbO_6$ has contributions from the $Q^2$ and $Q^6$ order terms. The involvement of the higher order terms of the Landau free energy expansion in phase transitions is considered to be an indication of an addition instability; often the presence of a nearby third phase. This additional instability is most likely associated with the presence of the second intermediate structure. The increased contribution from the higher order terms suggests the relative stability of these two phases becomes approximately equal near the changeover point.

### 3.2. Structural phase transitions of $Ba_2YTaO_6$

The $Ba_2LnMO_6$ ($M = Nb^{5+}$ and $Ta^{5+}$) niobates and tantalates adopt the rhombohedral intermediate where $Ln = La^{3+}$ or $Pr^{3+}$ while those with the heavier lanthanides ($Nd^{3+}$–$Dy^{3+}$) adopt the tetragonal symmetry. There are three main differences between $La^{3+}$ and $Pr^{3+}$ and the heavier lanthanides. The first of these is that they have less $f$-electrons with $La^{3+}$ and $Pr^{3+}$ having $f^0$ and $f^1$ configurations, respectively. They are also less electronegative than the other lanthanides [16] and have a larger ionic radii, 1.032 and 0.99 Å compared to 0.983–0.912 Å [17]. Studies of $Ba_2YTaO_6$ now become interesting since $Y^{3+}$ has a $f^0$ configuration, an electronegativity intermediate between $La^{3+}$ and $Pr^{3+}$ [16] and a ionic radii of 0.900 Å [17]. If the smaller number of $f$-electrons or electronegativities causes the $La^{3+}$ and $Pr^{3+}$ compounds to adopt a rhombohedral structure then $Ba_2YTaO_6$ would also be expected be rhombohedral. If, however, size is the critical factor $Ba_2YTaO_6$ is expected to be tetragonal.

Since $Ba_2YTaO_6$ is cubic at room temperature we have examined its structure at low temperature to establish the structure of the distorted variant. We found peak splitting consistent with tetragonal symmetry at and below 234 K indicating that a phase transition between tetragonal $I4/m$ and cubic $Fm\bar{3}m$ symmetry occurs at this temperature (see Figs. 6 and 7). This result is consistent with the previous work by Zurmühlen et al. [18] who also found that $Ba_2YTaO_6$ adopted tetragonal symmetry below room temperature using conventional X-ray diffraction. A plot of spontaneous tetragonal strain (calculated the same way as for the niobates in our previous work [1]) versus temperature is linear indicating that this continuous phase transition is second order in nature with a critical temperature of 254(2) K. This is significantly above the phase transition temperature indicated by the loss of splitting of the lattice parameters at around 242 K (see Fig. 8) again highlighting the limitation of using peak splitting to determine the precise temperature of a phase transition.

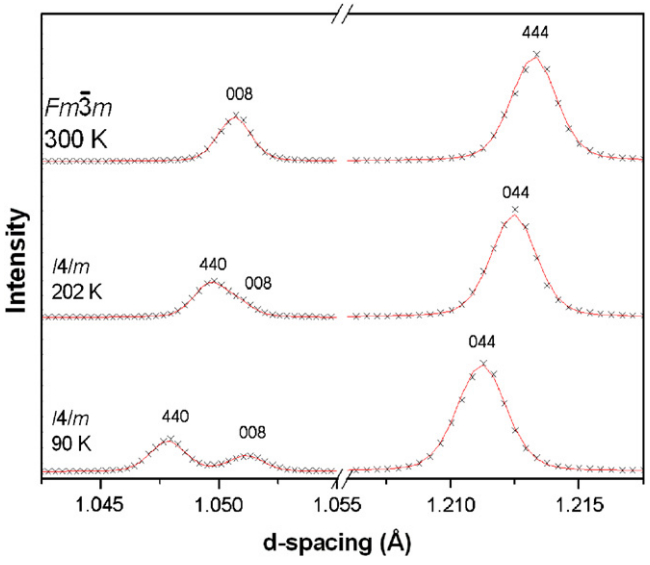


Fig. 6. Selected sections of the diffraction pattern for $Ba_2YTaO_6$ at various temperatures illustrating the tetragonal to cubic phase transition.

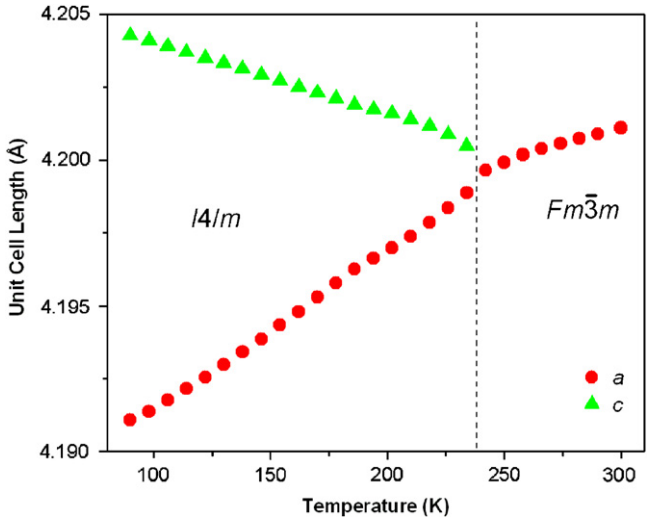


Fig. 7. Lattice parameters of $Ba_2YTaO_6$ with increasing temperature indicating the phase transition from tetragonal to cubic symmetry.

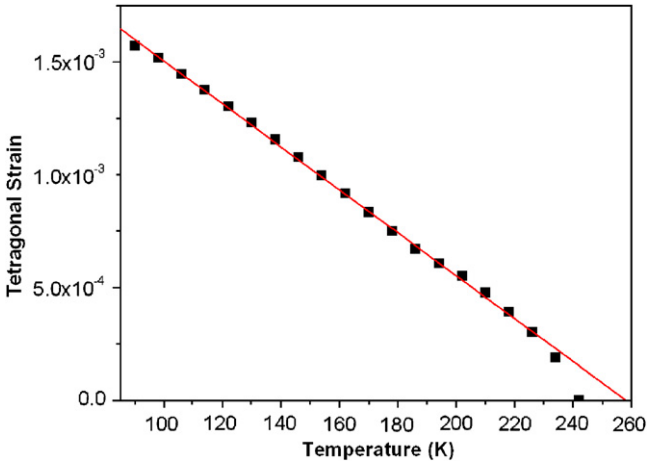


Fig. 8. Spontaneous tetragonal strain versus temperature for $Ba_2YTaO_6$. The linear nature of the plot indicates that the phase transition from tetragonal to cubic symmetry in this compound is second order.

That $Ba_2YTaO_6$ adopts tetragonal rather than rhombohedral symmetry demonstrates that the large ionic radii of $La^{3+}$ and $Pr^{3+}$ is the most significant factor causing tantalates and niobates with these cations to adopt rhombohedral symmetry. Why this should be so, is unclear although it may be related to the large size difference between the *B*-site cations. The rhombohedral structure may be favored by having a large difference between the volumes of the two *B*-site octahedra that is the size of these two cations. This size difference effect does not appear to be as significant as the $\pi$-bonding effects suggested previously [1] to be the reason why some series in the $Ba_2LnB'O_6$ ($B'$ = the common pentavalent cations) family adopt tetragonal, and others, rhombohedral symmetry. This is indicated by $Ba_2LnBiO_6$, which has the smallest size difference between $Ln^{3+}$ and $B'^{5+}$ cations adopting rhombohedral symmetry [8]. For the $Ba_2LnB'O_6$ perovskites both $\pi$-bonding and ionic radii clearly play a role in determining the intermediate symmetries adopted in other series factors such as electrostatic arrangement, tolerance factor and electronegativity, also play a crucial and often more significant role. In the case of the $Ba_2LnB'O_6$ family these other factors are such that the stability of the tetragonal and rhombohedral phases are similar so the nature of the $\pi$-bonding present and the size difference of the *B*-site cations can tip the balance for which symmetry is adopted.

## 4. Conclusion

This study has examined the structures of eight members of the series $Ba_2LnB'O_6$ ($Ln^{3+}$ = $La^{3+}$–$Sm^{3+}$ and $Y^{3+}$ and $B'$ = $Nb^{5+}$ and $Ta^{5+}$) using variable temperature synchrotron X-ray diffraction. Unlike the other niobate and tantalates studied to date $Ba_2LaB'O_6$ and $Ba_2PrB'O_6$ adopted $R\bar{3}$ rhombohedral symmetry as an intermediate phase between the $I2/m$ monoclinic and $Fm\bar{3}m$ cubic structures while the other compounds studied in this paper had the $I4/m$ tetragonal symmetry as the intermediate phase. In compounds near the point at which the change in intermediate symmetry occurs the temperature range over which the intermediate phase was stable was reduced and higher order parameters in the Landau free energy expansion contributed more to the phase transition. This is considered to indicate that the two intermediate phases approach equal stability in this region. That $Ba_2YTaO_6$ has tetragonal symmetry while the $La^{3+}$ and $Pr^{3+}$ compounds adopt a rhombohedral structure suggests that the $La^{3+}$ and $Pr^{3+}$ compounds have rhombohedral symmetry as a consequence of their larger ionic radii suggesting that the difference in size of the two *B*-type ionic radii is an important contributing factor.

## Acknowledgments

This work has been partially supported by the Australian Research Council and the Australian Institute of Nuclear Science and Engineering (AINSE) through the provision of an AINSE Postgraduate Award. The work performed at the Australian National Beamline Facility was supported by the Australian Synchrotron Research Program under the Major National Research Facilities program and was performed with the help of Dr. James Hester. The synchrotron radiation experiments were performed at the BL02B2 in the SPring-8 with the approval of the Japan Synchrotron Radiation Research Institute (JASRI) (Proposal no. 2007A1875).

## References

[1] P.J. Saines, B.J. Kennedy, M.M. Elcombe, J. Solid State Chem. 180 (2007) 401–409.
[2] P.J. Saines, M.M. Elcombe, B.J. Kennedy, Physica B 382 (2006).
[3] W.T. Fu, D.J.W. IJdo, J. Solid State Chem. 179 (2006) 1022–1028.
[4] W.T. Fu, D.J.W. IJdo, Solid State Communs. 136 (2005) 456–461.

[5] W.T. Fu, D.J.W. IJdo, J. Alloys Compd. 394 (2005) L5–L8.
[6] W.T. Fu, D.J.W. IJdo, J. Solid State Chem. 178 (2005) 2363–2367.
[7] E.J. Cussen, D.R. Lynham, J. Rogers, Chem. Mater. 18 (2006) 2855–2866.
[8] W.T.A. Harrison, K.P. Reis, A.J. Jacobson, L.F. Schneemeyer, J.V. Waszczak, Chem. Mater. 7 (1995) 2161–2167.
[9] A.M. Glazer, Acta Crystallogr. B 28 (1972) 3384–3392.
[10] A.M. Glazer, Acta Crystallogr. A 31 (1975) 756–762.
[11] P.J. Saines, J.R. Spencer, B.J. Kennedy, M. Avdeev, J. Solid State Chem., doi:10.1016/j.jssc.2007.08.009.
[12] T.M. Sabine, B.J. Kennedy, R.F. Garrett, G.J. Foran, D.J. Cookson, J. Appl. Crystallogr. 28 (1995) 513–517.
[13] E. Nishibori, M. Takata, K. Kato, M. Sakata, Y. Kubota, S. Aoyagi, Y. Kuroiwa, M. Yamakata, N. Ikeda, Nucl. Instrum. Methods Phys. Res. A 467/468 (2001) 1045–1048.
[14] B.A. Hunter, C.J. Howard, A Computer Program for Rietveld Analysis of X-ray and Neutron Powder Diffraction Patterns, Lucas Heights Laboratories, 1998.
[15] B.J. Kennedy, C.J. Howard, K.S. Knight, Z. Zhang, Q. Zhou, Acta Crystallogr. B 62 (2006) 537–546.
[16] K. Li, D. Xue, J. Phys. Chem. A 110 (2006) 11332–11337.
[17] R.D. Shannon, Acta Crystallogr. A 32 (1976) 751–767.
[18] R. Zurmühlen, E. Colla, D.C. Dube, J. Petzelt, I. Reaney, A. Bell, N. Setter, J. Appl. Phys. 76 (1994) 5864–5873.